Oxidation-enhanced annealing of implantation-induced $Z_{1/2}$ centers in 4H-SiC: Reaction kinetics and modeling

L. S. Løvlie and B. G. Svensson

University of Oslo, Department of Physics / Center for Materials Science and Nanotechnology, P.O. Box 1048 Blindern, N-0316 Oslo, Norway

(Received 10 May 2012; published 15 August 2012)

High-purity epitaxial layers of *n*-type 4H-SiC have been implanted with 4.3-MeV Si ions to a dose of 3×10^8 cm^{-2} and then subjected to dry isothermal oxidation at temperatures between 1050 and 1175 °C. Analysis of the samples by depth-resolved deep level transient spectroscopy unveils a strong oxidation-enhanced annealing of the prominent $Z_{1/2}$ center, commonly ascribed to the carbon vacancy. The integrated (total) loss of $Z_{1/2}$ centers is proportional to the thickness of the silicon dioxide (SiO_2) layer grown but the proportionality constant, or annihilation efficiency, decreases with decreasing oxidation temperature. At a given depth x, the annealing of $Z_{1/2}$ obeys first-order kinetics with a rate constant c having an activation energy of ∼5.3 eV. The pre-exponential factor c decreases with increasing x and a normalized concentration-versus-depth distribution of the species injected from the surface and annihilating the $Z_{1/2}$ centers has been deducted. This species is believed to be the carbon interstitial and is labeled C_I: numerical simulations of the reaction kinetics employing a model where (i) the generation rate of C_I at the SiO_2/SiC interface is related to the oxidation rate, (ii) the diffusion of C_I into the SiC layer is fast, and (iii) a steady-state concentration profile of C_I is rapidly established, yield good agreement with the experimental data for the evolution of both $Z_{1/2}$ (absolute values) and C_I (relative values) with temperature, depth, and time. The activation energy obtained for the diffusivity of C_I is ∼3.0 eV, presumably reflecting the migration barrier for C_I and possibly some contribution from an extra barrier to be surmounted at the SiO_2/SiC interface.

DOI: 10.1103/PhysRevB.86.075205 PACS number(s): 71.55.−i

I. INTRODUCTION

The most common polytypes of silicon carbide (SiC), 3C, 4H, and 6H, are gradually becoming attractive electronic materials in terms of high-quality bulk and epitaxially grown layers and also in terms of dopant and defect control. However, unlike most other semiconductors, the available methods for selective area doping of SiC are almost inherently restricted to ion implantation, due to the low diffusivity of most dopant elements.[1–3] This makes a genuine understanding of implantation-induced defects of paramount importance, in order to gain acceptable dopant activation and tailoring of the charge carrier lifetime in active parts of SiC devices. In particular, the prominent $Z_{1/2}$ center, which exhibits an acceptor-like level at about $E_C - 0.68$ eV in 4H-SiC (E_C denotes the conduction band edge),[4,5] has been shown to have a detrimental effect on the minority charge carrier lifetime.[6] $Z_{1/2}$ is typically present with concentrations on the order of 10^{12}–10^{13} cm^{-3} in as-grown material but can be reduced by high-temperature annealing, although a complete removal is challenging since $Z_{1/2}$ remains or even reforms at temperatures approaching 2000 °C.[7,8] Recently, however, several reports have shown that [$Z_{1/2}$] (brackets denote concentration values) can be reduced below the detection limit ($\leqslant 10^{10}$ cm^{-3}) in a surface layer by either a shallow carbon implantation followed by annealing at 1600 °C,[9] or, perhaps more conveniently, thermal oxidation performed on the Si-face at comparatively low temperatures (∼1100 °C).[10–12] Effectively, a "defect-free" layer with an extension of several tens of micrometers in thickness can be formed. In both cases, the removal of $Z_{1/2}$ was attributed to in-diffusion of a defect species, presumably the carbon interstitial (C_I), which reacts with and annihilates $Z_{1/2}$. Hence the atomic structure of $Z_{1/2}$ involves most likely a carbon vacancy (V_C).[13–17] Indeed, convincing evidence exists, obtained by different types of experiments, that $Z_{1/2}$ is carbon related.[10,14,17–19] This is also corroborated by modeling results based on density-functional-theory (DFT) where V_C and Si-C antisite pairs have been put forward as possible candidates for $Z_{1/2}$.[20–22]

Thermal oxidation of SiC resembles that of silicon but with the additional role of carbon: carbon can be (i) released in the form of CO and CO_2, (ii) incorporated and trapped in the growing layer of SiO_2, and/or (iii) accumulated at the SiO_2/SiC interface and injected into the bulk of SiC as C_I. In addition to the removal of $Z_{1/2}$, thermal oxidation leads also, via process (iii), to the formation of a donorlike defect with a level in the lower half of the band gap, detected in *p*-type material.[23] For both low- and high-dose implantations, this center can be annealed out at 1400–1500 °C under inert ambient conditions.[23]

In the present work, we have investigated the physical processes governing the enhanced annealing of $Z_{1/2}$ centers during oxidation. A nonuniform concentration-versus-depth distribution of $Z_{1/2}$ has been formed by low-fluence implantation of mega-electron-volt Si ions and the evolution of this distribution is monitored after isothermal treatment in dry oxygen atmosphere at temperatures in the range 1050–1175 °C. The relative depth distribution of the injected species, referred to as C_I, is determined together with the kinetics and activation energy of the annihilation process of $Z_{1/2}$. A first-order reaction is revealed with a decreasing rate constant as a function of depth, implying an almost time-independent (steady-state) concentration profile of C_I at a given temperature. The experimental data are compared with simulations, assuming a "simple" defect reaction model, and quantitative values for the generation rate, diffusivity, and migration energy of C_I are estimated.

II. EXPERIMENTAL

The material studied was *n*-type (0001) 4H-SiC, purchased from Cree Inc., with a 4° offcut angle and a 10 μm thick epitaxial layer grown by chemical vapor deposition on a highly *n*-doped substrate ($\sim 10^{18}$ cm^{-3}). The epitaxial layer was doped with nitrogen to an effective carrier concentration of $\sim 2.5 \times 10^{15}$ cm^{-3} as determined by capacitance-voltage (*C-V*) measurements. The samples were implanted with 4.3 MeV Si ions to a fluence of 3×10^8 cm^{-2}. The implants were performed in a direction close to the sample normal to minimize channeling, yielding a defect distribution peaking at $\sim$1.5–1.6 μm in depth. The concentration of $Z_{1/2}$ centers before implantation was 3×10^{12} cm^{-3} and uniformly distributed in the epitaxial layer, as measured by deep level transient spectroscopy (DLTS). Subsequently, the implanted samples were annealed in dry O_2 atmosphere at temperatures between 1050–1175 °C, and circular Schottky contacts with a diameter of 800 μm were formed by thermal evaporation of Ni after oxide removal in dilute hydrofluoric acid. In parallel, control samples were prepared under identical conditions except for annealing in dry N_2 (and not O_2) atmosphere. DLTS and *C-V* measurements were then employed to determine the concentration-versus-depth profiles of $Z_{1/2}$ and the charge carriers, respectively. For the measurements, an upgraded version of a custom made setup, described in detail elsewhere,[24] was used. Especially, the concentration-versus-depth profiles of $Z_{1/2}$ were obtained by selecting one rate window and holding the temperature constant at the maximum of the peak. The steady-state reverse bias voltage was kept constant, while gradually increasing the amplitude of the filling pulse (50 ms duration). The depth profiles were then extracted from the dependence of the recorded DLTS signal on the pulse amplitude, where the voltages used were converted into depth according to the conventional relations for Schottky contacts and accounting for the so-called λ effect.[25] The depth resolution is fundamentally limited by the Debye length, which equals $\sim$0.08 μm at 300 K in the epitaxial layers used. The absolute depth scale may suffer from systematic errors of the capacitance values recorded during the DLTS profiling measurements. However, these errors are estimated to be less than $\sim$10%, based on comparison between the peak position obtained for the $Z_{1/2}$ center after the implantation with 4.3 MeV ^{28}Si ions ($\sim$1.55 μm) and experimentally determined range distributions of MeV ions in 4H- and 6H-SiC[26] as well as simulated defect distributions using the TRIM code.[27]

III. DEFECT KINETICS: SOME BASIC CONSIDERATIONS

A defect species A, with concentration $[A] = [A](T,x,t)$, anneals according to a first-order process if the decay rate is proportional to $[A]$,

$$\frac{\partial [A]}{\partial t} = -c\,(T,x)\,[A], \tag{1}$$

where $c(T,x)$ is the decay constant, T is the absolute temperature, x is the sample depth, and t is the annealing time. This gives the exponential time dependence with the solution

$$[A]\,(T,x,t) = [A]_0 e^{-c(T,x)t}, \tag{2}$$

where $[A]_0$ is the concentration at $t = 0$ and $[A]$ is assumed to vanish at $t = \infty$. The decay constant $c(T,x)$ is typically represented on an Arrhenius form:

$$c(T,x) = c_0(x) e^{-E_a/kT}, \tag{3}$$

where c_0 is the frequency factor and E_a is the activation energy for the decay process.

In principle, there are three kinds of physical processes giving rise to first-order kinetics (see Ref. 28 and references therein): (i) dissociation where A disintegrates into its constituents while back reactions (association) are negligible, (ii) a reaction between A and a species B with a much larger concentration than A, and (iii) a reaction between A and a species B which is continuously replenished by a source such that $[B]$ remains constant as a function of time.

The rate of change in the concentration of defects involved in diffusion-limited reactions can be described by coupled partial differential equations,[29] and assuming the case (ii) or (iii) one obtains for A:

$$\frac{\partial [A]}{\partial t} = -4\pi R\,(D_A + D_B)\,[A][B] + D_A \frac{\partial^2 [A]}{\partial x^2}, \tag{4}$$

where R is referred to as the capture radius of the reaction with B, and D_A and D_B are the diffusivities of A and B, respectively. The first term on the right hand side of Eq. (4) describes the reaction rate between A and B, while the second one accounts for diffusion of A if a concentration gradient exists. Typically, one of the species is much more mobile than the other at a given temperature. Assuming $D_B \gg D_A$ and that $[B]$ remains essentially constant as a function of time, Eq. (4) becomes identical to Eq. (1) with $c(T,x) = 4\pi R D_B [B]$. Case (ii) ($[A] \ll [B]$) holds commonly for studies of irradiation-induced point defects interacting with oxygen in Czochralski-grown silicon, where $[O_I] \approx 10^{18}$ cm^{-3}, while the defect concentrations are typically at least one order of magnitude lower.[28] Case (iii) is more "exotic" and seldom found, since it requires a continuous supply of B in order to maintain a constant concentration as a function of time ($[B](t = 0) \approx [B](t = \infty)$ in spite of $[A]$ being comparable to $[B]$).

For case (ii), the temperature dependence of $c(T,x)$ is given by that of D_B,

$$D_B = D_\infty \exp\,(-E_d/kT)\,, \tag{5}$$

where D_∞ is the diffusivity at infinite temperature and E_d is the activation energy for diffusion. In case (iii), also a possible variation of $[B]$ with temperature needs to be accounted for and the deduced activation energy of $c(T,x)$ does not necessarily equal E_d.

IV. EXPERIMENTAL RESULTS

Figure 1 shows a representative selection of concentration-versus-depth profiles for the $Z_{1/2}$ level at $\sim E_C - 0.68$ eV after annealing at 1150 °C in N_2 and O_2 atmospheres. For the control samples (N_2 anneal), the profiles remain essentially identical and display a peak concentration of $\sim 6 \times 10^{14}$ cm^{-3} regardless of the duration (and temperature) used. In contrast, for the oxidized samples, $[Z_{1/2}]$ decreases with increasing time. The profiles peak at a depth of $\sim$1.55 μm and exhibit a

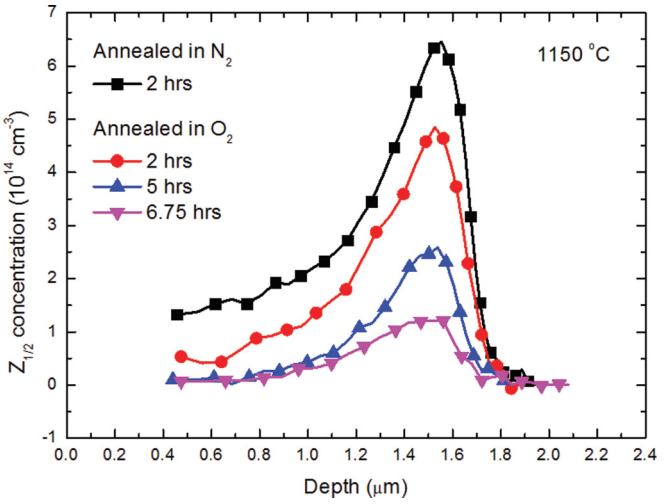

FIG. 1. (Color online) Concentration vs depth profiles of the $Z_{1/2}$ level, after annealing in O_2 and N_2 atmospheres at 1150 °C.

pronounced tail towards the surface, as anticipated after MeV ion implantation.[30] In addition to the decrease in absolute values also the shape of the profiles is altered during the oxidation showing a larger relative reduction in the surface tail than in the peak region.

In Fig. 2(a), the concentration of $Z_{1/2}$ at $x = 0.8$ μm is plotted as a function of the oxidation time at 1050, 1100, 1125, 1150, and 1175 °C. In each case, the decay of $[Z_{1/2}]$ exhibits an exponential dependence and the rate constant $c(T,x)$ increases strongly with temperature, cf. Eq. (2) with $A = Z_{1/2}$. Hence the annihilation process of $Z_{1/2}$ obeys first-order kinetics and $c(T,x)$ has been extracted at four different depths, x = 0.8, 1.0, 1.2, and 1.4 μm. The results are shown in Figure 2(b) as an Arrhenius plot with $c(T,x)$ is depicted versus the reciprocal absolute temperature; within the experimental accuracy, E_a stays constant as a function of x and a value of 5.4 ± 0.3 eV is obtained. However, the prefactor, $c_o(x)$, decreases with increasing x and is reduced by a factor of two between $x = 0.8$ and 1.4 μm. The absolute values of c_o, i.e., the intercept with the ordinate when T approaches infinity, carry a significant uncertainty, but are in the range of 10^{13} to 10^{16} s^{-1}.

Without oxidation, $Z_{1/2}$ persists up to temperatures of ∼2000 °C in irradiated samples[7] and it may even be thermally (re)generated above ∼1700 °C.[8] An activation energy of $\geqslant$8 eV has been estimated for the annealing of $Z_{1/2}$ assuming dissociation.[7] Thus during the oxidation E_a is lowered by ∼3 eV and dissociation can be ruled out as the controlling process. This conclusion is also substantiated by the variation of $c(T,x)$ with x; for a first-order dissociation process $c(T,x)$ depends only on T and not on x. Accordingly, the oxidation-enhanced annihilation process of $Z_{1/2}$ is either of the type (ii) or type (iii), as discussed in Sec. III.

Figure 3 shows the total loss of $Z_{1/2}$ centers, determined by integration of the depth profiles, as a function of thickness of the SiO_2 layer grown at 1050, 1100, 1125, 1150, and 1175 °C. The oxidation takes place in the parabolic time domain but for the temperatures and durations used the nonlinearity is weak and a linear dependence holds with a high degree of accuracy.[31] Figure 3 unveils a close proportionality with a slope having a tendency to increase with T, especially between 1125 and 1150 °C where the difference is a factor ∼2. These data demonstrate quantitatively the direct relation between the amount of oxidized Si atoms and the amount of annihilated $Z_{1/2}$ centers but also that the annihilation efficiency depends on T, i.e., it is not sufficient to consider only the thickness of the grown SiO_2 layer when estimating the amount of annihilated $Z_{1/2}$ centers.

V. DISCUSSION

A. Defect reaction model assumed for simulations

The decreasing annihilation rate of $Z_{1/2}$ with increasing depth (see Figs. 1 and 2) implies in-diffusion of an annihilating species from the SiC surface, in accordance with previous

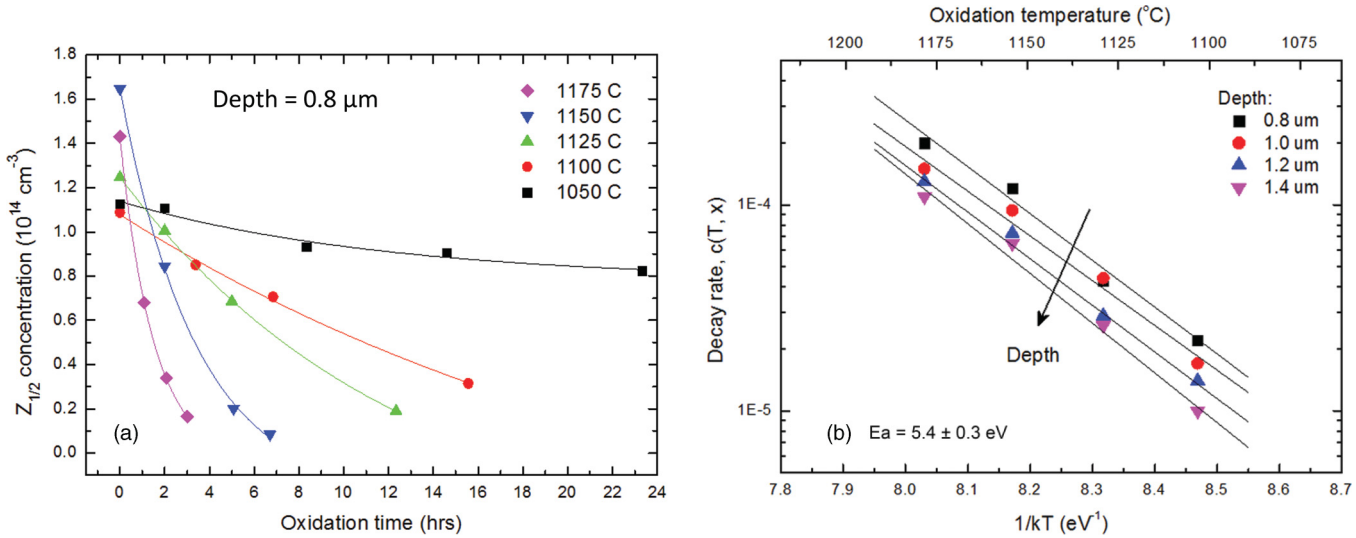

FIG. 2. (Color online) (a) The concentration of $Z_{1/2}$ at $x = 0.8$ μm as a function of the oxidation time. The lines are exponential fits of the measured values and show a close agreement. (b) The exponential decay rate of $[Z_{1/2}]$ at $x = 0.8$, 1.0, 1.2, and 1.4 μm vs the reciprocal absolute temperature. The decay rate decreases with x but the activation energy stays constant at 5.4 ± 0.3 eV.

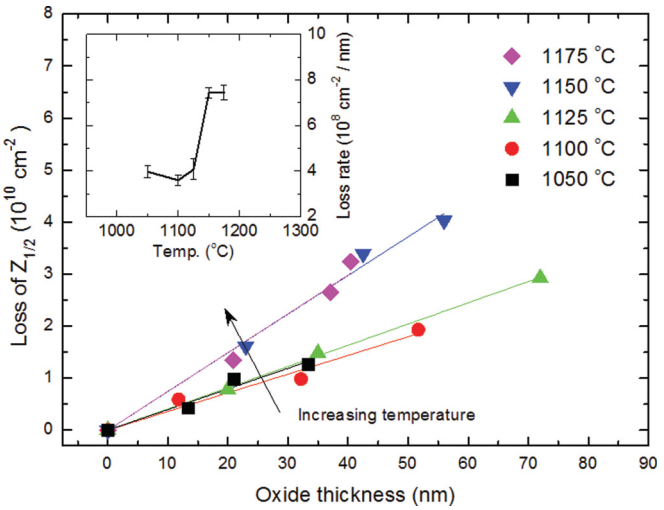

FIG. 3. (Color online) The loss of $Z_{1/2}$ per cm^{-2} as a function of the thickness of the grown SiO_2 layer. The inset shows the loss of $Z_{1/2}$ per nm of grown SiO_2 versus temperature.

findings in the literature.[11,12] Hereafter, this species will be referred to as C_I and it is generated during the oxidation process. However, an injection into the SiC bulk is not the only alternative for C_I; competing reactions exist and their relative importance increases with decreasing temperature (see Fig. 3). These reactions include trapping of C_I in the SiO_2 layer and at the SiO_2/SiC interface resulting in the formation of a Si-C-O interlayer and/or clusters of C.[32] Also out-diffusion of C_I through the SiO_2 surface may be considered but it is anticipated to decrease with t and no corresponding increase in the annihilation efficiency of $Z_{1/2}$ is observed experimentally. Hence, as a first approximation the following reaction model has been assumed,

$$C_I + Z_{1/2} \rightarrow \emptyset, \tag{6}$$

$$C_I + C_I \rightarrow C_2, \tag{7}$$

where the latter reaction accounts for the trapping of C_I via formation of immobile carbon dimers (C_2), primarily at the SiO_2/SiC interface but also in the SiO_2 and SiC layers. Further, $Z_{1/2}$ is regarded as immobile and applying Eq. (4), the differential rate equations for $Z_{1/2}$ and C_I become

$$\frac{\partial[Z_{1/2}]}{\partial t} = -4\pi R D_{C_I}[Z_{1/2}][C_I] \tag{8}$$

$$\frac{\partial[C_I]}{\partial t} = g - D_{C_i}\frac{\partial^2[C_I]}{\partial x^2} - 4\pi R D_{C_I}[C_I]([Z_{1/2}] + [C_I]). \tag{9}$$

g is the generation rate of C_I close the interface and put as

$$g \begin{cases} > 0, & 0 < x < 10 \text{ nm}, \\ = 0, & x > 10 \text{ nm}. \end{cases}$$

The width of 10 nm reflects the extension of the Si-C-O transition layer and g has a time evolution in accordance with that of the growth rate of the SiO_2 layer.[31] D_{C_I} is given by

$$D_{C_I} = \begin{cases} 1.6 \times 10^{-11}\text{cm}^2/\text{s} \ \ (\text{in } SiO_2), \\ \text{fitting parameter} \ \ (\text{in SiC}), \end{cases}$$

where the value in SiO_2 is taken from Ref. 30. For $[Z_{1/2}](T,x,t=0)$ the measured concentration-versus-depth profile in the control sample is used, while $[C_I](T,x,t=0)$ is put equal to zero. The model is schematically illustrated in Fig. 4 for an arbitrary time t. The SiO_2/SiC interface is treated as a reference plane at $x = L/2$ and the SiO_2 layer is held constant with a sufficient thickness (40 μm) to apply $[C_I](T,x=0,t) = 0$ as a boundary condition. Thus, as a first approximation, out-diffusion of C_I is omitted since the experimental data show minor (if any) variation of the annihilation efficiency of $Z_{1/2}$ with the thickness of the SiO_2 layer grown. Further, both $[Z_{1/2}]$ and $[C_I]$ are vanishing in the SiC bulk (large x values).

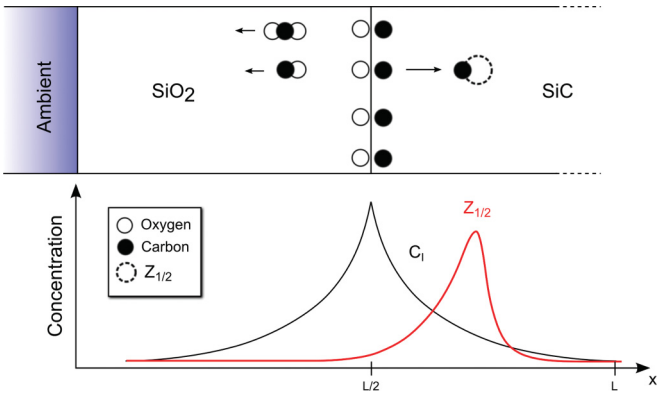

FIG. 4. (Color online) Schematic illustration of the model and sample structure assumed in the simulations.

B. Ultimate annihilation efficiency

In the ultimate limit of annihilation efficiency, every injected C_I contributes to the loss of $Z_{1/2}$, as assumed by the present authors in Ref. 12, and then the flux of C_I being emitted from the SiO_2/SiC interface can be extracted from the total loss of $[Z_{1/2}]$ versus t, Fig. 3. Such a treatment has been applied to all the experimental data for $[Z_{1/2}](T,x,t)$ and the extracted values of the flux were used as input to the simulations. D_{CI} was treated as a fitting parameter and varied until an optimum agreement with the measured depth profiles of $[Z_{1/2}]$ was obtained. The values deduced for D_{CI} are given in Fig. 5 and similar to that found in Ref. 12, where only one temperature was studied (1150 °C), they suggest a rapid diffusivity on the order of 10^{-8} cm^2/s. The variation with T is weak and in fact, opposite to that anticipated for a thermally activated process, i.e., D_{CI} decreases with increasing T. This suggests strongly that the basic assumption of the ultimate annihilation efficiency is not valid and a different approach needs to be taken.

C. Extraction of relative C_I profiles and modeling of both $Z_{1/2}(T,x,t)$ and $C_I(T,x,t)$

As shown by the experimental data, the annihilation of $Z_{1/2}$ exhibits first-order kinetics and the reaction process is either

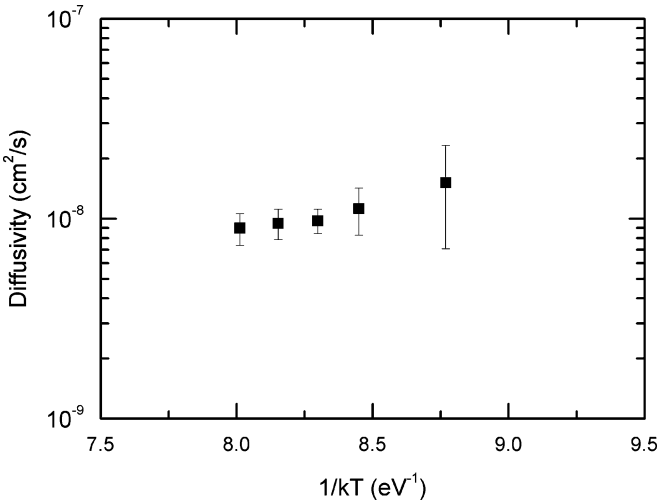

FIG. 5. The diffusivity of C_I vs the reciprocal absolute temperature deduced under the assumption that every injected C_I contributes to the loss of $Z_{1/2}$.

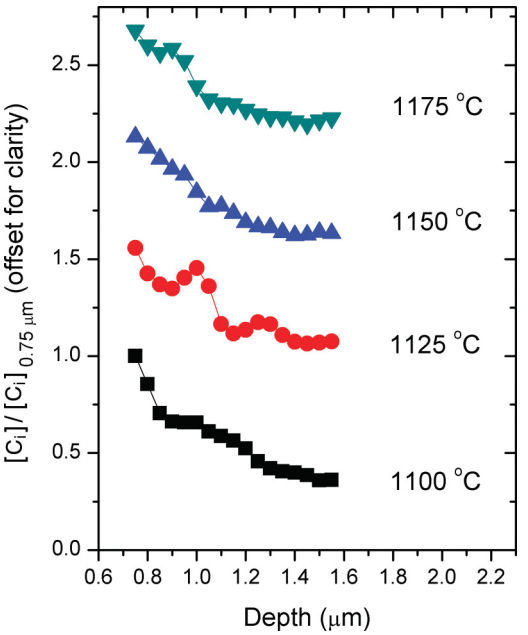

FIG. 6. (Color online) Depth profiles of $[C_I]'$ extracted from Eq. (11) for oxidation at 1100, 1125, 1150, and 1175 °C. The profiles are displaced along the y axis to improve the readability.

of type (ii) or (iii) (see Sec. III). Accordingly, from Eq. (8) the following relationship can be derived for $c(x)$ at a given temperature:

$$c(x) = 4\pi R D_{CI}[C_I](x,t), \tag{10}$$

where the time dependence of $[C_I]$ is negligible (the explicit temperature dependence of the quantities in Eq. (10) has been omitted for ease of reading). C_I is injected from the oxidizing surface and the depth dependence of the decay rate of $Z_{1/2}$, i.e., $c(T,x)$ in Figure 2(b), is due to the variation of $[C_I]$ with x. A large $[C_I]$ gives fast decay of $Z_{1/2}$, which therefore is high at the surface and decreases towards the bulk. The relative depth profile of $[C_I]$ ($[C_I]'$), e.g., normalized to $[C_I]$ at (or close to) the surface, can be extracted from Eq. (10) by realizing that

$$[C_I]' = \frac{[C_I](x)}{[C_I](x_{surf})} = \frac{c(x)}{c(x_{surf})}. \tag{11}$$

We have used $x_{surf} = 0.75\ \mu$m, which is the most shallow depth where $[Z_{1/2}]$ is sufficiently large for an accurate determination of $c(x)$. The extracted distributions of $[C_I]'$ are depicted in Fig. 6 and a clear decrease with x is revealed at all the oxidation temperatures employed. The distributions extend up to $x = 1.6\ \mu$m, i.e., just beyond the peak position of $[Z_{1/2}]$, whilst at larger depths, the rapid decrease of $[Z_{1/2}]$ prevents an accurate extraction.

The profiles of $[C_I]'$ in Fig. 6, and their negligible variation with t, imply one more criteria to be fulfilled by the simulations in addition to the evolution of $[Z_{1/2}]$ with T, x, and t. For each oxidation temperature and duration, g and D_{CI} have been varied independently to fit both $[Z_{1/2}](x)$ and $[C_I]'$ (x) by solving Eqs. (8) and (9). The results of such a fitting procedure are illustrated in Fig. 7 for oxidation at 1100 °C, where the squared sum of the difference between simulated and experimental data is depicted in D_{CI}-versus-g plots for $[C_I]$' [see Fig. 7(a)] and $[Z_{1/2}]$ [see Fig. 7(b)]. Corresponding results have also been obtained for the other temperatures (not shown). In the fitting, D_{CI} was held constant as a function of t, while g displayed a weak decrease during the initial stage, in accordance with a parabolic time domain of the oxidation process. Further, in the SiO_2 layer, D_{CI} has been taken from Hijikata *et al.*[33] and is anticipated to have low activation energy (~0.5–0.6 eV), i.e., it stays almost constant in the temperature range studied. The absolute value of D_{CI} in the SiO_2 layer carries, however, an uncertainty by a few orders of magnitude [34] and, especially, higher values than that used in the simulations (1.6×10^{-11} cm^2/s) may be anticipated, as suggested by Krafcsik *et al.*[35] A diffusivity of 10^{-10} cm^2/s shifts the plots in Fig. 7 by a factor of ~2 towards higher g values but with minor effects on the topology.

As unveiled by Fig. 7(a), the solutions for C_I are rather selective with respect to D_{CI} but not to g. However, the solutions for $Z_{1/2}$ are selective to both g and D_{CI}, Fig. 7(b), and combining the results for C_I and $Z_{1/2}$ one obtains $D_{CI} \approx 1 \times 10^{-12}$ cm^2/s and $g \approx 1{-}2 \times 10^{13}$ cm^{-3}s^{-1} as the optimum values at 1100 °C. These values are not fully unique but are estimated to be valid within a factor of two for D_{CI} and less than a factor of 10 for g (albeit subject to change depending on D_{CI} in SiO_2 as discussed above). Figure 8 shows Arrhenius plots for g and D_{CI} determined at 1100, 1125, 1150, and 1175 °C, where also the physical condition of the activation energy (E_a) of g equal to, or above, that of the oxidation process has been imposed. $E_a(g)$ equals ~3.3 eV, which is slightly higher than the value of ~3.1 eV obtained for the oxidation rate (not shown). The latter value is identical with that reported previously for oxidation of the Si(0001) face by Song *et al.*[31] The values in Fig. 8 give a good agreement between the simulations and the experimental data of $[Z_{1/2}](T,x,t)$ and $[C_I]'$ (T,x,t), as demonstrated in Figs. 9(a) and 9(b) for 1100 and 1175 °C, respectively, where the simulations are represented by solid curves and the measurements by data points (symbols). Here, it should be emphasized that only

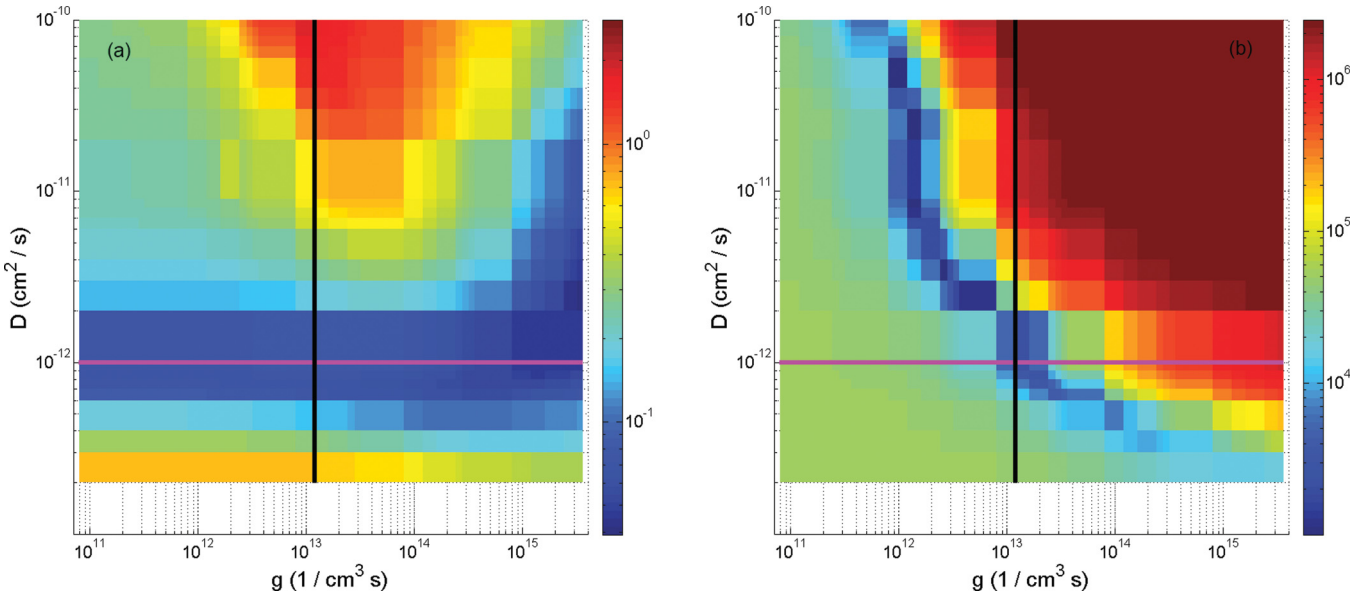

FIG. 7. (Color online) The squared deviation of the simulated data compared with the experimentally determined depth profiles of (a) C_I' and (b) $Z_{1/2}$ after oxidation at 1100 °C. The intersection of the pink and black lines represents the optimal combination of D_{CI} and g.

a relative comparison holds for C_I since only normalized values of $[C_I]$ ($[C_I]'$) can de deduced from the experiments [cf. Eq. (11)]. In Fig. 9, $[C_I]'(T,x,t)$ has been multiplied by a constant factor, given by the ratio between the simulated value of $[C_I](T,x = 0.8\ \mu m,t)$ and $[C_I]'(T,x = 0.8\ \mu m,t)$, in order to facilitate the comparison with the simulated $[C_I](T,x,t)$ distributions.

$E_a(g) \approx 3.3$ eV implies a lowering by at least 4 eV for the generation of "free" C_I's at the SiO_2/SiC interface compared to the formation energy estimated for C_I in bulk SiC under equilibrium conditions,[36] and it illustrates the strong catalytic effect of the oxidation process. $E_a(D_{CI}) \approx 3.0$ eV is ascribed to the migration energy of the free C_I's injected to the SiC layer; this value is ~2.0 eV higher than the migration barrier predicted by Bockstedte *et al.* [36] for C_I in the energetically favorable split-interstitial configuration. The calculations in Ref. 33 were performed for the 3C-polytype but are expected to provide a first insight also into the diffusion processes in other polytypes, like 4H. The difference of ~2.0 eV may indicate that the free C_I's have to surmount an additional energy barrier at the SiO_2/SiC interface before migrating rapidly into the SiC layer. On the other hand, it can also be noted that self-diffusion experiments of ^{12}C and ^{13}C in intrinsic 4H-SiC yielded the activation energy for the diffusion of C, which was ~1.5–2.0 eV higher than that obtained in Ref. 33 for an interstitial mechanism.

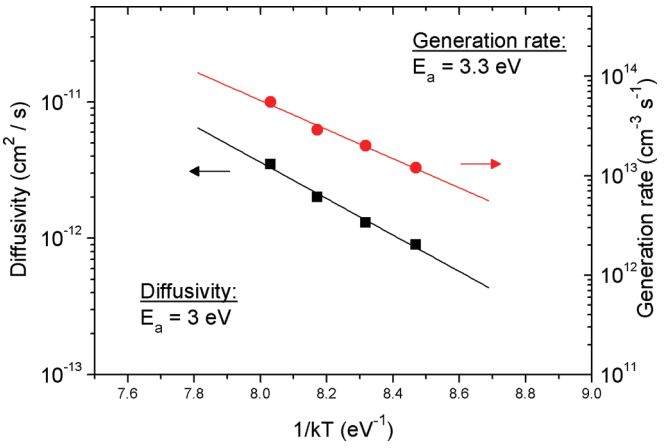

FIG. 8. (Color online) The values of D_{CI} and g extracted from the simulations vs the reciprocal oxidation temperature.

The sum of $E_a(g)$ and $E_a(D_{CI})$ equals ~6.3 eV, which is ~0.9 eV higher than the value extracted for the decay rate, c, of $Z_{1/2}$, see Fig. 2(b). This shows a weaker increase of $[C_I]$ with T (lower E_a) than that of g, as c is directly proportional to $[C_I]$ for a given D_{CI} [see Eq. (10)]. Further, the shape of the simulated $[C_I]$-versus-depth profiles stays approximately the same for the different T's (see Fig. 9), consistent with the $[C_I]'$ profiles in Fig. 6. Moreover, in spite of the annihilation with $Z_{1/2}$, $[C_I](T,x,t)$ remains almost constant as a function of t, i.e., the flux of C_I from the oxidizing surface is sufficiently high to maintain nearly a steady-state concentration. In fact, the weak time dependence of $[C_I](T,x,t)$ is a key feature for the apparent first-order annealing kinetics of $Z_{1/2}$ at a given depth, and referring to Sec. III, the exotic case (iii) applies. The implantation-induced distribution of $[Z_{1/2}]$ can be regarded as a trapping (or barrier) layer for C_I to penetrate before reaching the bulk and the evolution of $[Z_{1/2}](T,x,t)$ is a monitor of the flux of C_I's. Accordingly and consistent with Fig. 3, the integrated loss of $[Z_{1/2}]$ for a given thickness of grown SiO_2 decreases with decreasing oxidation temperature since the integrated flux of C_I's does not only hinge on the amount of generated C_I's but also on their diffusivity, cf. Eq. (10) where the decay rate of $Z_{1/2}$ includes both $[C_I]$ and D_{CI}.

Finally, one can notice that the estimated values of g are minute relative to the rate of oxidized Si atoms at the SiO_2/SiC interface with a difference of 5–6 orders of magnitude. Hence,

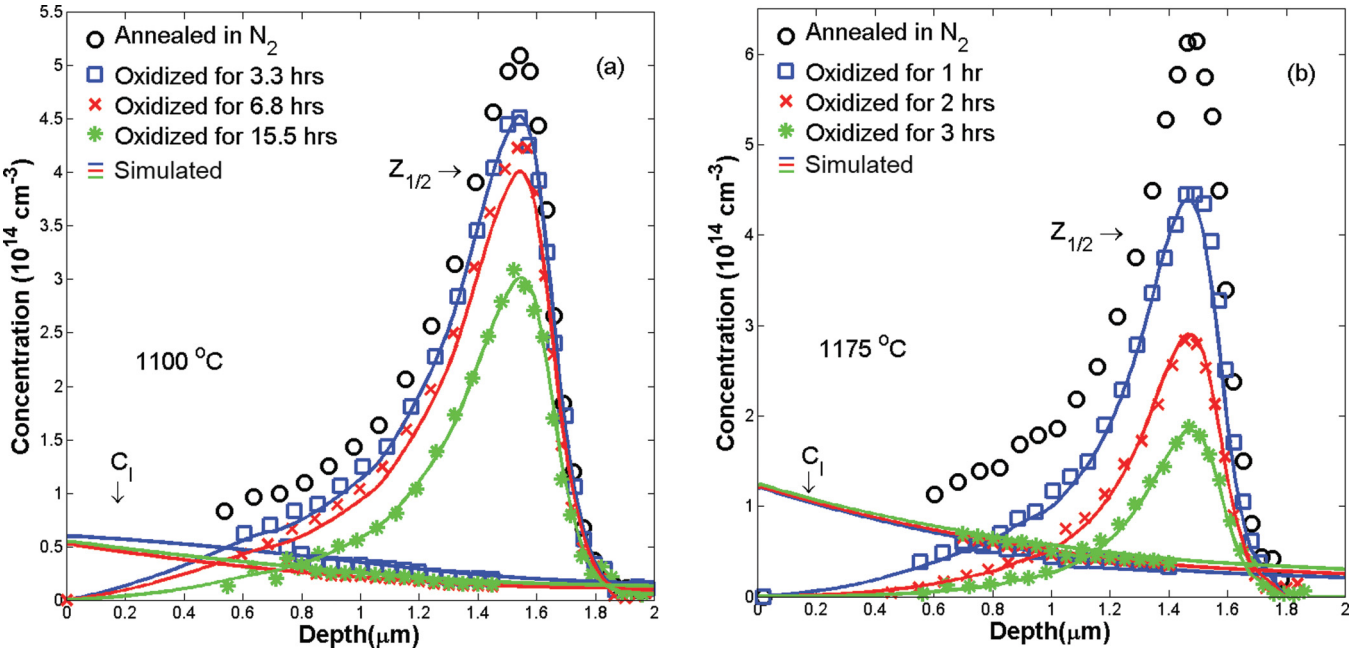

FIG. 9. (Color online) The temporal evolution of the $Z_{1/2}$ and C_I concentration-versus-depth profiles at (a) 1100 °C and (b) 1175 °C, with activation energies of 3.0 eV for D_{CI} and 3.3 eV for g. $[C_I]$ stays nearly time-independent through-out the $Z_{1/2}$ profiles, yielding first-order annealing kinetics of $Z_{1/2}$ at a given depth. Experimental data are represented by symbols and calculated data by solid curves.

oxidation-induced injection of C_I is an important process for bulk defects but not the prevailing one at the SiO_2/SiC interface. Moreover, on the basis of the g values only a few percent of the injected C_I's are estimated to annihilate with $Z_{1/2}$, which is substantially lower than the ultimate limit of 100% discussed (and ruled out) in Sec. V B.

VI. CONCLUSIONS

At a given depth x, oxidation-induced annihilation of $Z_{1/2}$ centers in the parabolic time regime obeys first-order kinetics with a rate constant $c(T,x)$ having an activation energy of ~5.4 eV. The pre-exponential factor of $c(T,x)$ decreases with increasing x, which suggests a decreasing steady-state concentration of the annihilating species, C_I, injected from the SiO_2/SiC interface. The experimental data for $Z_{1/2}(T,x,t)$ and $[C_I]'(T,x,t)$ can be quantitatively described by a "simple" kinetic model (schematically illustrated in Fig. 4) where g is essentially proportional to the oxidation rate and D_{CI} is fast, while $Z_{1/2}$ is immobile as corroborated by data for control samples annealed in N_2 atmosphere. The absolute values extracted for D_{CI} and g are not fully unique but are expected to be valid within a factor 2 and 10, respectively. D_{CI} exhibits an activation energy of ~3.0 eV, presumably reflecting the migration barrier of C_I with possibly some addition from a barrier to be surmounted at (or in the vicinity of) the SiO_2/SiC interface before reaching the SiC layer. The simulations suggest a rapid establishment of steady-state concentration-versus-depth profiles of C_I and this is a key feature in order to account for the observed first-order annealing kinetics of $Z_{1/2}$. Moreover, the total loss of $Z_{1/2}$ centers is found to be proportional to the thickness of the SiO_2 layer grown. However, the proportionality constant (annihilation efficiency) decreases with decreasing T and according to the modeling results, this can primarily be attributed to the decrease of D_{CI} at low T.

ACKNOWLEDGMENTS

Fruitful discussions with Dr. Hijikata are highly appreciated, and financial support from the Norwegian Research Council (FRINATEK program) is gratefully acknowledged.

[1]M. S. Janson, M. K. Linnarsson, A. Hallén, B. G. Svensson, and N. Nordell, Appl. Phys. Lett. **76**, 1434 (2000).
[2]L. J. Kroko and A. G. Milnes, Solid State Electron. **9**, 1125 (1966).
[3]R. J. Trew, J.-bang Yan, and P. M. Mock, Proc. IEEE **79**, 598 (1991).
[4]C. Hemmingsson, N. T. Son, O. Kordina, J. P. Bergman, E. Janzen, J. L. Lindstrom, S. Savage, and N. Nordell, J. Appl. Phys. **81**, 6155 (1997).
[5]T. Dalibor, G. Pensl, T. Kimoto, H. Matsunami, S. Sridhara, R. P. Devaty, and W. J. Choyke, Diam. Relat. Mater. **6**, 1333 (1997).
[6]P. B. Klein, B. V. Shanabrook, S. W. Huh, A. Y. Polyakov, M. Skowronski, J. J. Sumakeris, and M. J. O'Loughlin, Appl. Phys. Lett. **88**, 52110 (2006).
[7]G. Alfieri, E. V. Monakhov, B. G. Svensson, and M. K. Linnarsson, J. Appl. Phys. **98**, 43518 (2005).
[8]B. Zippelius, A. Glas, H. B. Weber, G. Pensl, T. Kimoto, and M. Krieger, Mat. Sci. Forum (in Press, 2012) (n. d.).
[9]L. Storasta and H. Tsuchida, Appl. Phys. Lett. **90**, 062116 (2007).
[10]T. Hiyoshi and T. Kimoto, Appl. Phys. Express **2**, 41101 (2009).

[11]T. Hiyoshi and T. Kimoto, Appl. Phys. Express **2**, 91101 (2009).
[12]L. S. Løvlie and B. G. Svensson, Appl. Phys. Lett. **98**, 052108 (2011).
[13]N. T. Son, X. T. Trinh, L. S. Løvlie, B. G. Svensson, K. Kawahara, J. Suda, T. Kimoto, T. Umeda, J. Isoya, T. Makino, T. Ohshima, and E. Janzén (unpublished).
[14]L. Storasta, J. P. Bergman, E. Janzén, and A. Henry, J. Appl. Phys. **96**, 4909 (2004).
[15]J. Zhang, L. Storasta, J. P. Bergman, N. T. Son, and E. Janzen, J. Appl. Phys. **93**, 4708 (2003).
[16]C. G. Hemmingsson, N. T. Son, A. Ellison, J. Zhang, and E. Janzén, Phys. Rev. B **58**, R10119 (1998).
[17]T. Kimoto, S. Nakazawa, K. Hashimoto, and H. Matsunami, Appl. Phys. Lett. **79**, 2761 (2001).
[18]K. Danno and T. Kimoto, J. Appl. Phys. **100**, 113728 (2006).
[19]T. Kimoto, K. Hashimoto, and H. Matsunami, Jpn. J. Appl. Phys. **42**, 7294 (2003).
[20]T. A. G. Eberlein, C. J. Fall, R. Jones, P. R. Briddon, and S. Öberg, Phys. Rev. B **65**, 184108 (2002).
[21]T. Hornos, A. Gali, and B. G. Svensson, Mater. Sci. Forum **679–680**, 261 (2011).
[22]L. Torpo, M. Marlo, T. E. M. Staab, and R. M. Nieminen, J. Phys.: Condens. Matter **13**, 6203 (2001).
[23]K. Kawahara, J. Suda, G. Pensl, and T. Kimoto, J. Appl. Phys. **108**, 033706 (2010).
[24]B. G. Svensson, K.-H. Ryden, and B. M. S. Lewerentz, J. Appl. Phys. **66**, 1699 (1989).
[25]S. D. Brotherton, Solid State Electron. **26**, 987 (1983).
[26]M. S. Janson, M. K. Linnarsson, A. Hallén, and B. G. Svensson, J. Appl. Phys. **93**, 8903 (2003).
[27]J. Ziegler, www.srim.org (2010).
[28]B. G. Svensson and J. L. Lindström, Phys. Rev. B **34**, 8709 (1986).
[29]T. R. Waite, Phys. Rev. **107**, 463 (1957).
[30]G. Alfieri, E. V. Monakhov, B. G. Svensson, and A. Hallen, J. Appl. Phys. **98**, 113524 (2005).
[31]Y. Song, S. Dhar, L. C. Feldman, G. Chung, and J. R. Williams, J. Appl. Phys. **95**, 4953 (2004).
[32]S. T. Pantelides, S. Wang, A. Franceschetti, R. Buczko, M. D. Ventra, S. N. Rashkeev, L. Tsetseris, M. H. Evans, I. G. Batyrev, L. C. Feldman, S. Dhar, K. McDonald, R. A. Weller, R. D. Schrimpf, D. M. Fleetwood, X. J. Zhou, J. R. Williams, C. C. Tin, G. Y. Chung, T. Isaacs-Smith, S. R. Wang, S. J. Pennycook, G. Duscher, K. V. Benthem, and L. M. Porter, Mater. Sci. Forum **527–529**, 935 (2006).
[33]Y. Hijikata, H. Yaguchi, and S. Yoshida, Appl. Phys. Express **2**, 021203 (2009).
[34]Y. Hijikata (private communication).
[35]O. H. Krafcsik, G. Vida, I. Pocsik, K. V. Josepovits, and P. Deák, Appl. Phys. **40**, 2197 (2001).
[36]M. Bockstedte, A. Mattausch, and O. Pankratov, Phys. Rev. B **68**, 205201 (2003).